Formation and coupling of magnetic moments in Heusler alloys

J. Kübler
Technische Hochschule Darmstadt, Institut für Festkörperphysik, D-6100 Darmstadt, West Germany

A. R. Williams
IBM Thomas J. Watson Research Center, Yorktown Heights, New York 10598

C. B. Sommers
Laboratoire de Physique des Solides, Bâtiment 510, F-91401 Orsay, France
(Received 14 March 1983)

The microscopic mechanisms responsible for both the formation and coupling of magnetic moments in Heusler alloys (X_2MnY) are identified. We find that the X atoms (e.g., Cu, Pd) serve primarily to determine the lattice constant, while the Y atoms (e.g., Al, In, Sb) mediate the interaction between the Mn d states. There is no significant direct interaction between the Mn atoms, but the occupied d states of Mn are delocalized by their strong interaction with the X-atom d states. The localized character of the magnetization results from the *exclusion* of minority-spin (defined locally) electrons from the Mn $3d$ shell. The coupling between the localized magnetic Mn moments can be described with the Heisenberg Hamiltonian and the sign of the exchange constants results from a competition between the intra-atomic magnetic energy and interatomic Y-atom mediated covalent interactions between the Mn d states. These effects compete because the covalent mechanism is possible only for antiferromagnetic alignments, but necessarily reduces the magnitude of the local moments. The sensitive dependence of magnetic order on the occupation of the mediating p-d hybrid states accounts well for experiments by Webster in which this occupation is varied by alloying. Our analysis is based on self-consistent, spin-polarized energy-band calculations for Co_2MnAl, Co_2MnSn, Ni_2MnSn, Cu_2MnAl, Cu_2MnSn, Pd_2MnIn, Pd_2MnSn, and Pd_2MnSb, for both ferromagnetic and antiferromagnetic spin alignments.

I. INTRODUCTION

Heusler alloys[1-3] are ternary, magnetic, intermetallic compounds, usually containing Mn, with $L2_1$ crystal structure and are defined by the generic formula X_2MnY with X=Co, Ni, Cu, Pd, etc., and Y=Al, Sn, In, Sb, etc. When the elements X and Y are nonmagnetic, the magnetization is essentially confined to the Mn sublattice. When the element X is Co or Ni an additional magnetization appears at the Co or Ni sites.[4]

Heusler alloys are traditionally considered to be ideal local-moment systems.[5,6] Consequently, one uses the Heisenberg Hamiltonian to describe the ordering of the moments and discusses the exchange constants in terms of indirect Ruderman-Kittel-Kasuya-Yosida–type (RKKY-type) exchange mediated by the free electrons of the systems.[7-11] Neutron-scattering measurements[5,12,13] of the spin-wave spectra of Ni_2MnSn, Pd_2MnSn, and Cu_2MnAl have led to a detailed knowledge of the exchange-interaction constants, and, at least for the case of Pd_2MnSn, a fit of the measured exchange constants with theoretical formulas has been quite successful.[10,11] The chemical trend in the evolution of the ferromagnetic state has been illustrated by measurements of Webster and coworkers[14,15] on the systems $Pd_2MnIn_cSb_{1-c}$ and $Pd_2MnIn_cSn_{1-c}$; these show impressively how the magnetic coupling changes as the conduction-electron concentration is changed.

Our principal objective here is to point out that the physical picture of these systems differs from that usually employed in the discussion of magnetic order. By carrying out energy-band calculations for a series of Heusler alloys we succeed in establishing an understanding of the strength of the magnetic coupling which varies considerably in the systems studied here, ranging from weakly antiferromagnetic in Pd_2MnIn to strongly ferromagnetic in Co_2MnSn. The picture that emerges from these calculations is that of *delocalized* d electrons moving in a common d band formed by the d states of the Mn atoms and those of the X atoms. Yet the calculations indicate that the magnetization is very much confined to the Mn atoms. The localized character of the magnetization results from the *exclusion* of minority-spin (defined locally) electrons from the Mn $3d$ shell.

The results of our energy-band calculations differ only in quantitative detail from earlier calculations by Ishida *et al.*[16-18] The important differences between the present and earlier work are (1) our effort to establish chemical trends by performing calculations for many systems, i.e., Co_2MnAl, Co_2MnSn, Ni_2MnSn, Cu_2MnAl, Cu_2MnSn, Pd_2MnIn, Pd_2MnSn, and Pd_2MnSb, (2) the minimization of the total energy to obtain the volume, (3) the direct calculation of the total-energy difference between the ferromagnetic and antiferromagnetic moment alignments, and (4) the present calculations are self-consistent. They are based on the local-spin-density treatment of electronic exchange and correlation[19-21] and on the augmented-spherical-wave[22] formalism for the solution of the effective single-particle equations. Parts of this work were reported previously.[23]

In Sec. II we give details of the electronic structure of the Heusler alloys and show how the localized magnetic moments are formed. In Sec. III we discuss the coupling of the local moments on different Mn atoms and explain chemical trends in the energy that stabilizes the ferromagnetic state. In this section we also obtain Heisenberg exchange constants which allow one to estimate the paramagnetic Curie temperatures. In Sec. IV we summarize our conclusions.

II. FORMATION OF MOMENTS

Four sets of calculations[24] were done for the Heusler alloys Co_2MnAl, Cu_2MnAl, Co_2MnSn, Ni_2MnSn, Cu_2MnSn, Pd_2MnIn, Pd_2MnSn, and Pd_2MnSb; these were (1) nonmagnetic, (2) ferromagnetic (F), (3) antiferromagnetic type I (AF I), and (4) antiferromagnetic type II (AF II). The different types of ordering and the crystal structure are illustrated in Fig. 1. AF I is characterized by alternating planes parallel to the (001) plane, AF II by alternating planes parallel to the (111) plane of up- and down-spin moments.[25] Figure 1 also shows the p orbitals of a Y atom in X_2MnY: They couple moments of the same direction in AF I but of opposite direction in AF II. This is important because we will find that p-d hybrid states constitute the effective coupling of d states on different Mn atoms.

Figure 2 shows some of our state-density results for assumed nonmagnetic X_2MnSn with X=Co, Ni, and Cu. The Fermi-level state density is due to both Mn *and* Co d states in Co_2MnSn but is entirely due to Mn d states in Cu_2MnSn and in all cases it well exceeds the critical (Stoner) value that is indicated in Fig. 2.

Minimization of the total energy with respect to both the volume and the magnetic order leads to the ground states of the Heusler alloys; all are found to have calculated ferromagnetic ones except for Pd_2MnIn which has an AF II ground state. This is in agreement with experiment.[14] State densities are given in Fig. 3 for X_2MnAl (X=Co and Cu), in Fig. 4 for X_2MnSn (X=Co, Ni, and Cu), and in Fig. 5 for Pd_2MnY (Y=In, Sn, and Sb). Here ↑ designates the majority-spin electrons and ↓ the minority-spin electrons; in AF II Pd_2MnIn, ↑ and ↓ are for one sublattice only. The minority-spin state densities

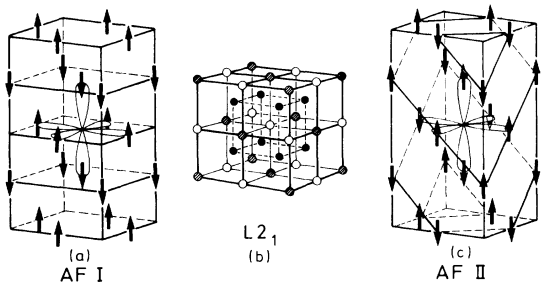

FIG. 1. Antiferromagnetic configuration of the first kind (a) and the second kind (c) in the fcc lattice. Mn spin-up and spin-down sublattices and the p orbitals in X_2MnY of the central Y atom are shown. Center: (b) $L2_1$ crystal structure, shaded circles, Mn; open circles, Y; solid black circles, X.

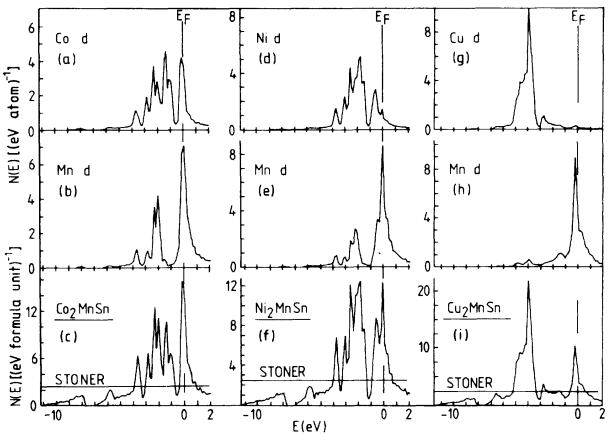

FIG. 2. Total state densities per formula unit of assumed nonmagnetic Co_2MnSn, Ni_2MnSn, and Cu_2MnSn shown in lower panels. Site- and angular-momentum-projected d-state densities of the constituents shown in upper panels.

at the Fermi energy for ferromagnetic Co_2MnAl and Co_2MnSn nearly vanish. This should lead to peculiar transport properties in these two Heusler alloys. Table I contains some ground-state quantities like lattice constants, heats of formation, and magnetic moments. Comparison of the calculated lattice constants with the experimental ones shows that the former are nearly always somewhat smaller then the measured ones. This may be due to the fact that most, if not all, of the lattice constants were measured at elevated temperatures. The heats of formations ΔH were obtained from the total-energy differences between the magnetic compounds and the constitu-

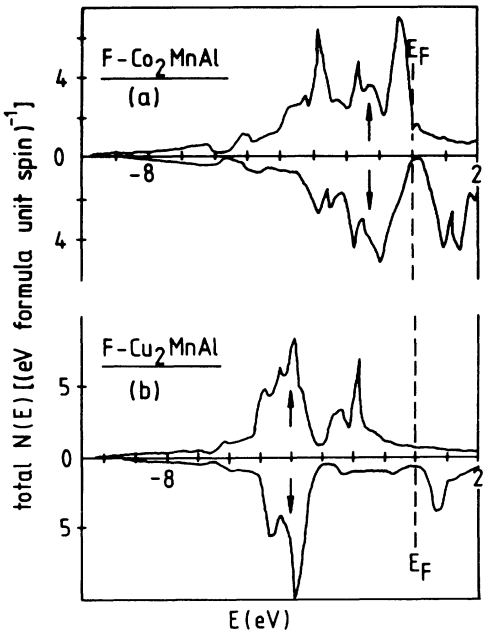

FIG. 3. Total majority (↑) and minority (↓) state densities per formula unit for ferromagnetic (a) Co_2MnAl and (b) Cu_2MnAl.

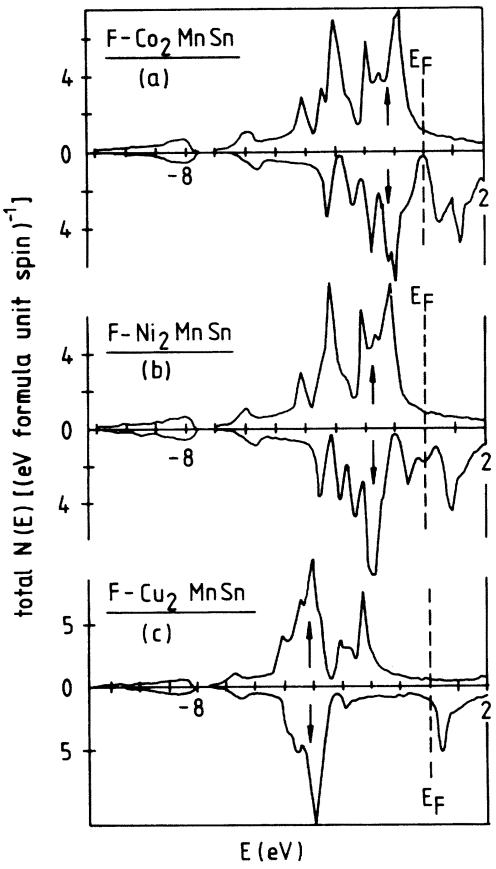

FIG. 4. Total majority (↑) and minority (↓) state densities for ferromagnetic (a) Co_2MnSn, (b) Ni_2MnSn, and (c) Cu_2MnSn.

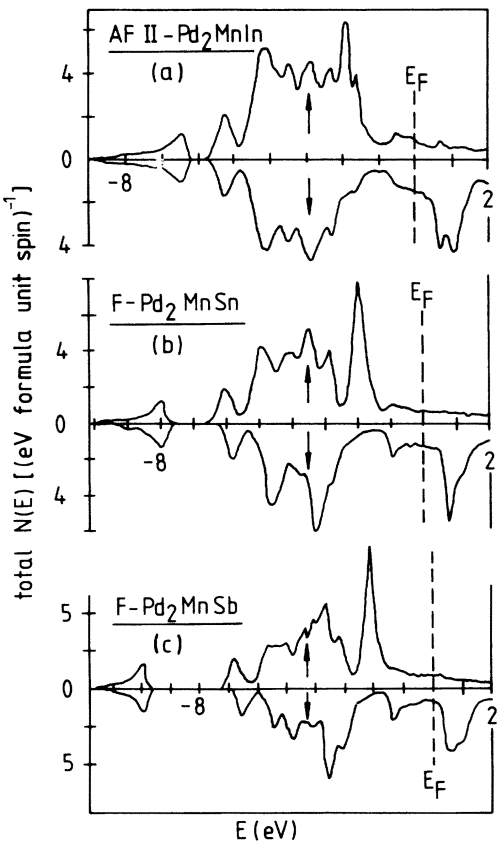

FIG. 5. Total majority (↑) and minority (↓) state densities for one sublattice of antiferromagnetic (a) Pd_2MnIn and for ferromagnetic (b) Pd_2MnSn, and (c) Pd_2MnSb.

ent metals. The calculated saturation moments μ_0 are the sum of the Mn spin moment plus the X and Y spin moments of one molecule X_2MnY. Except for the Co systems (where they agree with experiment) they are smaller than the measured ones, which may be due to orbital contributions not included in our calculations.

A decomposition of the state densities which clarifies the origin of a great deal of the peak structures seen in Figs. 3–5 is given in Figs. 6–13 which show the minority d-state densities of Mn and X in the lower part and the

TABLE I. Calculated and experimental lattice constants of ferromagnetic (AF II in the case of Pd_2MnIn) Heusler alloys, calculated heats of formation ΔH, calculated magnetic moments of Mn in Heusler alloys μ_{Mn}, and calculated and experimental saturation moments, μ_0^{calc} and μ_0^{expt}. Total sublattice moment of Pd_2MnIn is $4.04\mu_B$ (Ref. 14).

X_2MnY	a_{calc} (Å)	a_{expt} (Å)[a]	ΔH (eV)	μ_{Mn} (μ_B)	μ_0^{calc} (μ_B)	μ_0^{expt} (μ_B)
F-Co_2MnAl	5.68	5.76	−1.55	2.74	4.05	4.01±0.05[b]
F-Cu_2MnAl	5.85	5.95	−0.35	3.36	3.38	3.6–4.1[c,d]
F-Co_2MnSn	5.95	6.00	−0.79	3.13	5.02	5.08±0.05[b]
F-Ni_2MnSn	5.99	6.05	−0.93	3.39	3.75	4.05[c]
F-Cu_2MnSn	6.13	6.17	+0.3	3.52	3.61	4.11[c]
AF II-Pd_2MnIn	6.37	6.37	−0.98	3.90	0	0[e]
F-Pd_2MnSn	6.35	6.38	−1.60	3.78	3.86	4.23±0.1[e]
F-Pd_2MnSb	6.34	6.42	−1.54	3.83	4.0	4.4±0.1[e]

[a]All measured lattice constants from Campbell (Ref. 3).
[b]Webster (Ref. 4).
[c]Campbell (Ref. 3).
[d]Oxley *et al.* (Ref. 26) and Endo *et al.* (Ref. 27).
[e]Webster and Ramadan (Ref. 14).

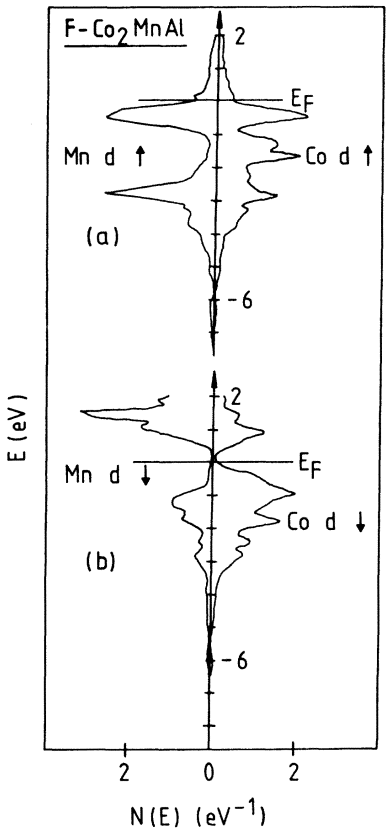

FIG. 6. Site- and spin-projected d-electron state densities for ferromagnetic Co_2MnAl.

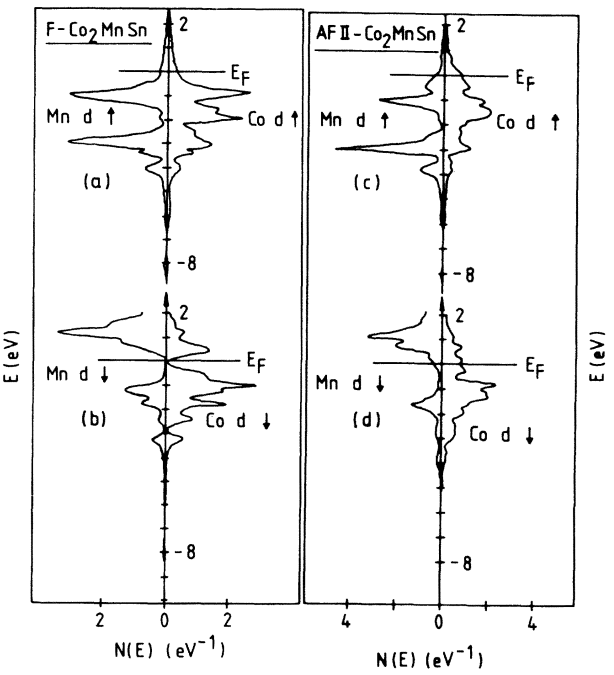

FIG. 8. Site- and spin-projected d-electron state densities for (a) and (b) ferromagnetic Co_2MnSn, and (c) and (d) antiferromagnetic Co_2MnSn.

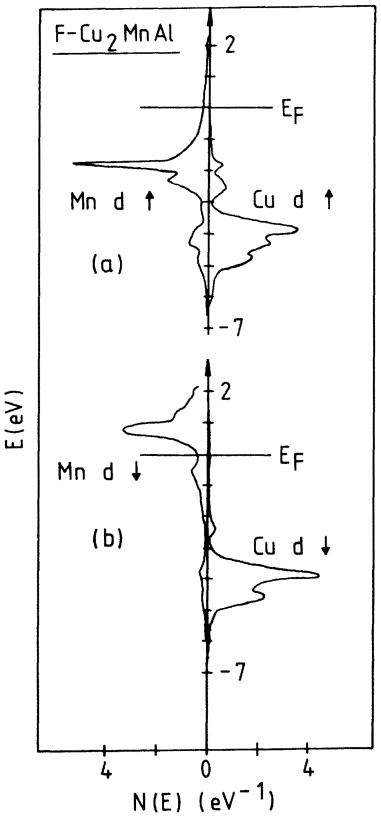

FIG. 7. Site- and spin-projected d-electron state densities for ferromagnetic Cu_2MnAl.

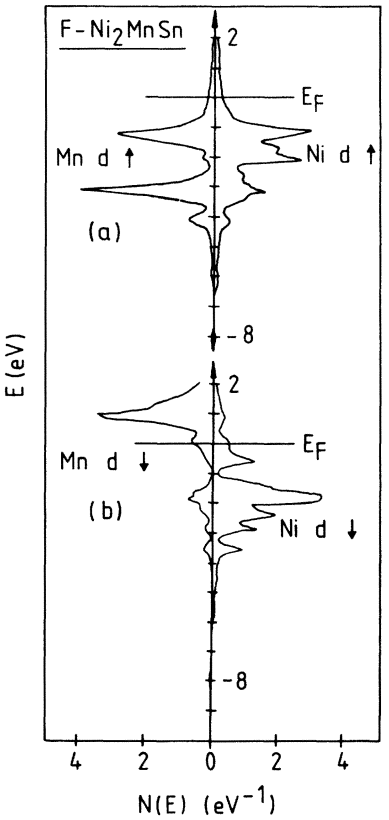

FIG. 9. Site- and spin-projected d-electron state densities for ferromagnetic Ni_2MnSn.

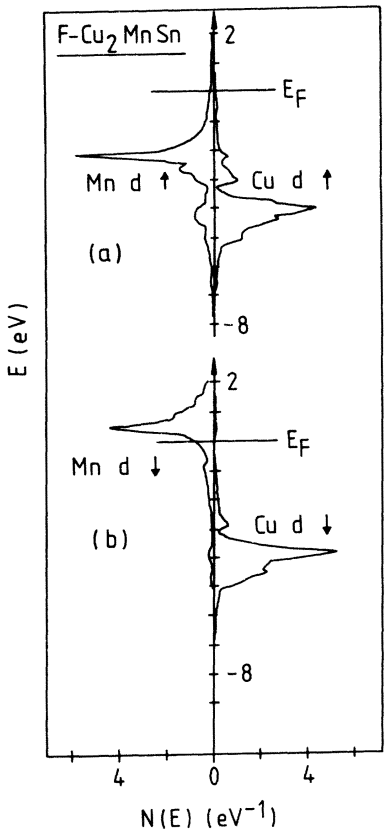

FIG. 10. Site- and spin-projected d-electron state densities for ferromagnetic Cu_2MnSn.

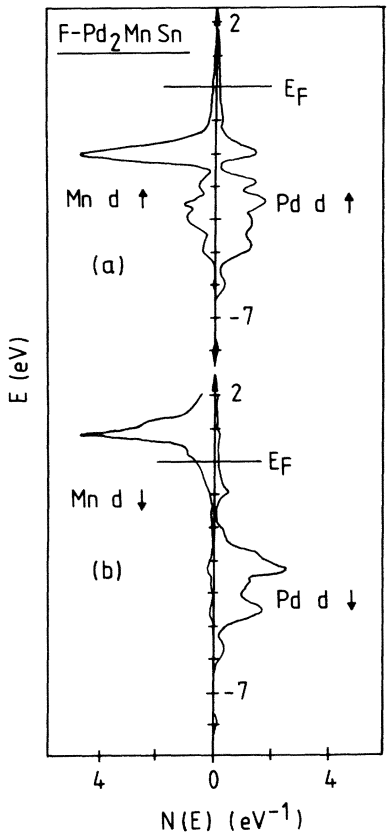

FIG. 12. Site- and spin-projected d-electron state densities for ferromagnetic Pd_2MnSn.

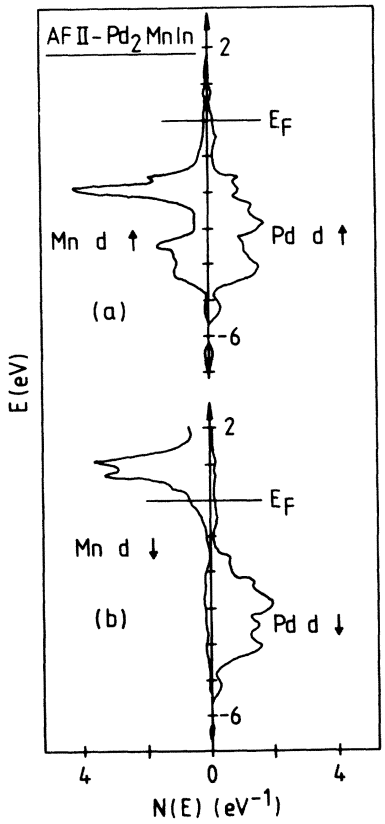

FIG. 11. Site- and spin-projected d-electron sublattice state densities for antiferromagnetic (AF II) Pd_2MnIn.

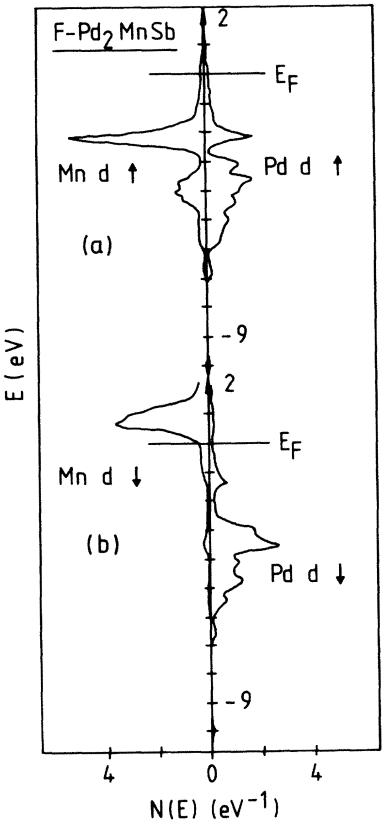

FIG. 13. Site- and spin-projected d-electron state densities for ferromagnetic Pd_2MnSb.

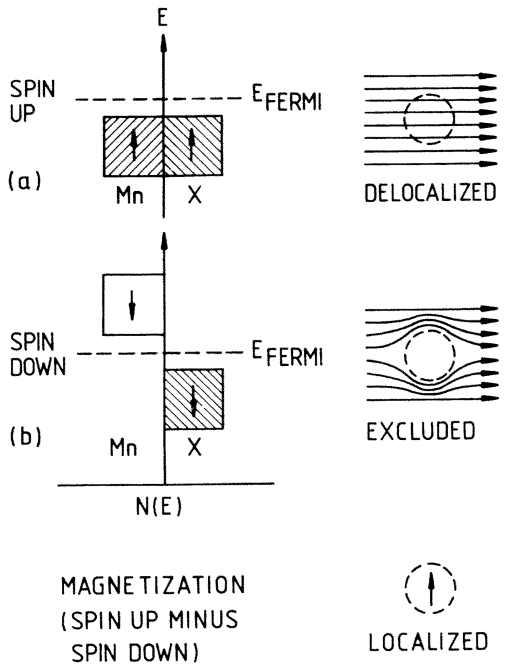

FIG. 14. Localized magnetic moment from delocalized electrons. Schematic diagram of up-spin and down-spin d electrons in Heusler alloys (X_2MnY). Corresponding nonschematic state densities are shown in Figs. 6–13.

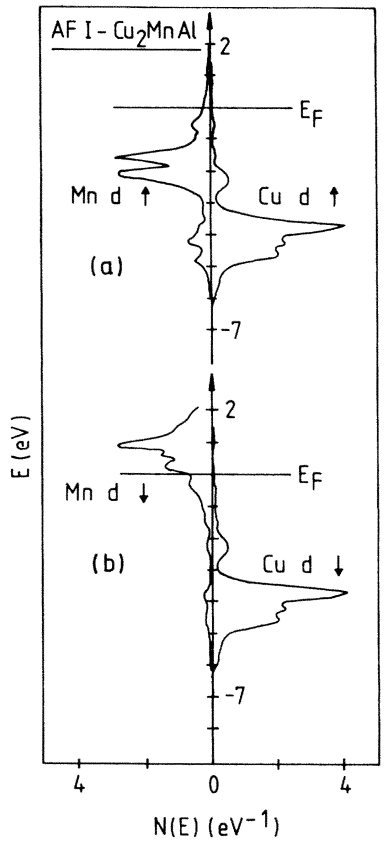

FIG. 15. Site- and spin-projected d-electron sublattice state densities for assumed antiferromagnetic (AF I) Cu_2MnAl.

majority d-state densities in the upper part, except for antiferromagnetic Pd_2MnIn where the d-state densities of one sublattice are shown (the other sublattice has ↑ and ↓ reversed).

The content and interpretation of Figs. 6–13 are described schematically in Fig. 14. The Mn spin-up d states are almost completely occupied and the bandwidths indicate that they are just as delocalized as the d electrons of Co, Ni, Cu, or Pd. The Mn spin-down states, however, are nearly empty, particularly in the Cu and Pd systems, including antiferromagnetic Pd_2MnIn. Put differently, the spin-up d electrons of the Mn atoms join those of the X atoms in forming a common d band, whereas the spin-down d electrons are almost completely *excluded* from the Mn sites. The results of this localized exclusion is an equally localized region of magnetization. We therefore have completely localized magnetic moments composed of completely itinerant electrons.

The notion of localized magnetic moments implies that their coupling can be described by the Heisenberg Hamiltonian. Before we show in Sec. III that this is indeed true for the Heusler alloys, we here turn to a more basic prerequisite required of local moments, namely that they remain intact when their direction is reversed. Figure 15 gives the d-state densities of AF I Cu_2MnAl for one sublattice; it should be compared with the ferromagnetic results given in Fig. 7. Except for details, which we will explore in Sec. III, both state densities are very much alike and so are the magnetic moments. Table II contains a

TABLE II. Magnetic moments of Mn atoms in μ_B for ferromagnetic, μ_{ferro}, AF I, $\mu_{AF\,I}$, and AF II, $\mu_{AF\,II}$, moment alignments. Total-energy differences ΔE_I between ferromagnetic and AF I moment alignments, and ΔE_{II} between ferromagnetic and AF II moment alignments, are also shown.

X_2MnY	μ_{ferro}	$\mu_{AF\,I}$	$\mu_{AF\,II}$	ΔE_I (meV)	ΔE_{II} (meV)
Co_2MnAl	2.74	3.0	2.97	−195.9	−157.8
Cu_2MnAl	3.36	3.26	3.19	−123.1	−183.7
Co_2MnSn	3.13	3.26	3.21	−268.7	−244.9
Ni_2MnSn	3.39	3.35	3.35	−81.6	−57.1
Cu_2MnSn	3.52	3.36	3.39	−38.1	−59.9
Pd_2MnIn	3.87	3.89	3.90	−13.6	+6.8
Pd_2MnSn	3.78	3.80	3.79	−82.5	−55.1
Pd_2MnSb	3.83	3.82	3.78	−1.4	−20.4

TABLE III. Occupation numbers q_l of s, p, and d bands in Heusler alloys for majority- ($\uparrow$) and minority- ($\downarrow$) spin electrons. Numbers are for calculated ground states—all ferromagnetic except for Pd_2MnIn, which is AF II. The latter occupation numbers are for one sublattice only. f-state contributions are 0.3—0.4 (not listed). Last two columns are Fermi-level state densities in eV^{-1}.

X_2MnY	$(q_s)_\uparrow$	$(q_p)_\uparrow$	$(q_d)_\uparrow$	$(q_s)_\downarrow$	$(q_p)_\downarrow$	$(q_d)_\downarrow$	$[N(E_F)]_\uparrow$	$[N(E_F)]_\downarrow$
Co_2MnAl	1.35	1.76	12.78	1.37	1.92	8.57	1.4	0.2
Cu_2MnAl	1.48	1.93	14.16	1.50	1.99	10.73	0.5	0.7
Co_2MnSn	1.42	2.09	13.32	1.40	2.18	8.25	1.0	0.1
Ni_2MnSn	1.45	2.10	13.65	1.44	2.17	9.86	0.9	2.0
Cu_2MnSn	1.55	2.24	14.36	1.54	2.25	10.77	0.5	1.2
Pd_2MnIn	1.39	1.79	13.64	1.37	1.76	9.67	0.8	1.3
Pd_2MnSn	1.44	2.00	13.79	1.43	2.11	9.86	0.6	1.2
Pd_2MnSb	1.51	2.37	13.90	1.47	2.41	9.93	0.8	1.0

compilation of the calculated magnetic Mn moments for F, AF I, and AF II moment alignments together with the total-energy differences, $\Delta E_{\rm I}$ and $\Delta E_{\rm II}$, between the ferromagnetic and antiferromagnetic alignments,

$$\Delta E_{\rm I} = E_{\rm tot}(\text{ferro}) - E_{\rm tot}(\text{AF I}) ,$$

$$\Delta E_{\rm II} = E_{\rm tot}(\text{ferro}) - E_{\rm tot}(\text{AF II}) .$$

The AF II state total energy is lowest in Pd_2MnIn only; here the magnetic moments are slightly larger for the antiferromagnetic alignments than for the ferromagnetic one. For the Co and Ni systems and for Pd_2MnSn the AF II state total energy is lower than the AF I energy. The antiferromagnetic moments are larger than the ferromagnetic ones in these systems, too, except for Ni_2MnSn. For the remaining systems the AF I state total energy is lower than the AF II energy. In these cases the antiferromagnetic moments are somewhat smaller than the ferromagnetic ones.

In Table III, finally, the distributions of occupation numbers over angular momenta is given together with Fermi-level state densities. It is only Cu_2MnAl for which we found a value of the coefficient γ of the electronic specific heat.[28] Its value implies a Fermi-level state density of 2.8 states per eV, which is about a factor of 2 larger than the calculated value. The same discrepancy was found by Ishida *et al.*[16] who suggested that spin fluctuations may cause an enhancement of γ.

III. COUPLING OF MOMENTS

The preceding discussion is concerned with the formation of localized magnetic moments on individual Mn atoms. We turn now to the question of the alignment of the moments of different Mn atoms. We do this in two parts: In subsection A we discuss and explain chemical trends, and in subsection B we determine Heisenberg exchange constants.

A. Trends

Our physical picture of the "exchange interaction" coupling the Mn moments is based on the results of Sec. II. One unequivocal conclusion of these results is that there is no significant direct interaction between the d states on different Mn atoms. Such an interaction, if present, would manifest itself in several ways in the state densities shown in Figs. 6—13 and 15. For example, if the direct interaction of Mn d states were significant, then the unoccupied Mn d band would be noticeably narrower in the case of antiferromagnetic alignments; a comparison of Fig. 7 with Fig. 15 shows that this is not so. The partial state densities indicate that the d states of different Mn atoms do interact, but only by using the states at the Y atoms as an intermediary. This can be seen by comparing again Fig. 7 with Fig. 15 and noticing the additional peak in the antiferromagnetic Mn $d\downarrow$ state density (Fig. 15) just above E_F which is not present in the ferromagnetic state density (Fig. 7); similarly, spectral weight is shifted in the Mn $d\uparrow$ state density below E_F when the alignment is changed from ferromagnetic to antiferromagnetic. The connection of these peaks with the Al p states is established by Fig. 16 which shows the minority Al p and Mn d states of AF II Cu_2MnAl on the left-hand side and those of Cu_2MnSn on the right-hand side (notice the peaks above E_F marked with a horizontal line). These p-d hybrid states are further illustrated by Fig. 17 which shows the minority p and d states of Y and Mn for antiferromagnetic Pd_2MnY, with Y=In, Sn and Sb. The variation of

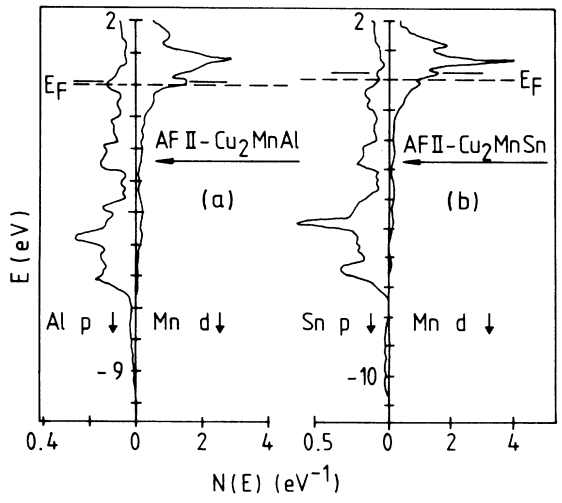

FIG. 16. Minority-site- and spin-projected state densities of p and d electrons of Al and Mn, respectively, in (a) antiferromagnetic Cu_2MnAl and of Sn and Mn, respectively, in (b) antiferromagnetic Cu_2MnSn.

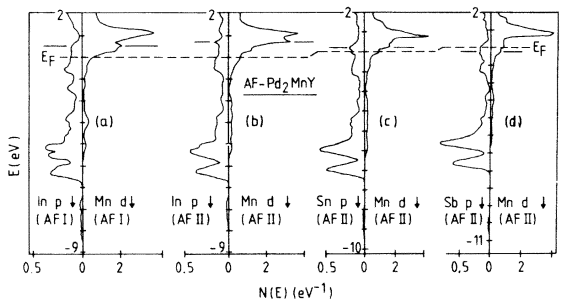

FIG. 17. Minority-site- and spin-projected state densities of p and d electrons in antiferromagnetic Pd_2MnY. From left to right: Y=In in AF I order then in AF II order; Y=Sn in AF II order; Y=Sb in AF II order.

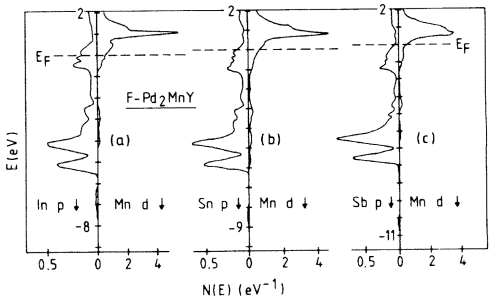

FIG. 18. Minority-site- and spin-projected state densities of p and d electrons in ferromagnetic Pd_2MnY for Y=In, Sn, and Sb (from left to right).

the strengths of the hybrids with different antiferromagnetic alignments is apparent from the left-hand side of Fig. 17. A similar plot for ferromagnetic Pd_2MnY, shown in Fig. 18, shows that these hybrid states are absent in this case.

Our interpretation of this observation is that the total-energy difference between the ferromagnetic and antiferromagnetic moment alignments results from a competition between two physical mechanisms, the intra-atomic exchange splitting of the Mn d states, and the interatomic covalent interaction of d states on different Mn atoms mediated by the p states of the Y constituent. These mechanisms both possess the important property of affecting the energies of states throughout the Mn d band. The involvement of d states well away from E_F is particularly visible in the case of the exchange energy, where it is manifest in the quadratic dependence of the exchange energy $\frac{1}{4}I\mu^2$ on the full local magnetization μ. (I is the intra-atomic exchange integral.) Whereas the magnetic energy applies equally to the ferromagnetic and antiferromagnetic alignments, the covalency mechanism[23,29] benefits only the *antiferromagnetic* alignment (see Figs. 17 and 18). This is because the *inter*atomic interactions couple only electrons of the same spin and are only effective in lowering the total energy if the states involved lie both above and below the Fermi energy. (The covalency mechanism lowers the energy of bonding hybrids and raises the energy of antibonding hybrids; if both are occupied, there is little net effect.) So, if the exchange energy benefits both alignments and the covalency mechanism benefits only the antiferromagnetic alignment, why are most Heusler alloys ferromagnetic? The answer is that an intrinsic part of the covalency mechanism is the mixture of states on different atoms to form the hybrid states, and this, in the present context, implies the population of minority-spin states, and therefore the reduction of the local magnetization and the loss of exchange energy. Thus, an intrinsic aspect of the covalency mechanism is a loss of local magnetization, and this, in our view, is the essence of the antiferromagnetic-ferromagnetic competition.

Our calculations suggest that in terms of the formula X_2MnY, the principal role of the X atoms is to determine the lattice constant. The Y atoms provide the p orbitals that mediate the covalent Mn-Mn interactions. The Y atoms, through their valence, also determine the extent to which the hybrid p-d orbitals are filled and thereby determine the moment-loss "price" associated with the covalency benefit. This role of the Y atoms is beautifully illustrated by the measurements of Webster and coworkers[14,15] which show the evolution toward the ferromagnetic state to be *twice* as rapid in the alloy system $Pd_2MnIn_cSb_{1-c}$ as in the system $Pd_2MnIn_cSn_{1-c}$. Indeed, Fig. 17 shows that the p-d hybrid states cross the Fermi energy, being far above in Pd_2MnIn and just below in Pd_2MnSb. The fact that Cu_2MnAl, despite Al's valence of three, is strongly ferromagnetic both experimentally and calculationally, might seem inconsistent with this rigid-band-theoretic interpretation of the role of the Y constituent. Rather, this example points out the limitations of rigid-band theory; it is appropriate for the description of small changes in chemical identity, as in the $Pd_2MnIn_cSb_{1-c}$ and $Pd_2MnIn_cSn_{1-c}$ systems, but it is not a useful guide to understanding larger chemical changes, such as those between Cu_2MnAl and Pd_2MnIn. In Cu_2MnAl the small lattice constant amplifies the mediated Mn-Mn covalent interactions and with them the loss of moment ($0.1\mu_B$; see Table II) in the antiferromagnetic state, causing the strong energetic preference for the ferromagnetic alignment.

Consider now the stability of the ferromagnetic spin alignment in the case of Ni-based Heusler alloys and the tremendous stability of the ferromagnetic alignment in the case of the Co-based alloys (see Table II). Figure 8 clearly reveals the source of this stability. We see in Fig. 8 that whereas the d states of Cu and Pd lie almost entirely below the Fermi level (see Figs. 10–13) in the Heusler alloys, those of Ni, and particularly those of Co, do not. The covalent interaction between the d states of Co and Ni and those of Mn is not markedly stronger than the analogous interaction in the Cu- and Pd-based Heusler alloys; the important difference between the Co- and Ni-based alloys on the one hand and the Cu- and Pd-based alloys on the other is the fact that a significant fraction of the antibonding hybrid states formed by this covalent interaction lie above the Fermi level in the case of the Co- and Ni-based alloys (see Figs. 8 and 9). So, where the metalloid atoms provide the important Mn-to-Mn coupling in the Cu- and Pd-based Heusler alloys, it is the more numerous

Co and Ni atoms that perform this role in the Co- and Ni-based alloys. When the Mn-Mn interaction is mediated by the X sublattice (generic Heusler formula X_2MnY), the interaction is ferromagnetic; if the interaction is mediated by the Y sublattice, it can have either sign, depending on the position of the Fermi level in the Mn-Y p-d hybrid states.

B. Heisenberg exchange constants

We finally turn to a discussion of the Heisenberg exchange constants in Heusler alloys. Since we argue that the magnetic moments are localized we *postulate* that the coupling of the moments on different Mn atoms can be described by the Heisenberg Hamiltonian

$$H=-\sum_{i,j} J_{ij}\vec{S}_i\cdot\vec{S}_j \ , \tag{1}$$

with exchange constants J_{ij} ($J_{ii}=0$). (We will ignore the Ni and Co moments.) The exchange energy in the ferromagnetic ground state at $T=0$ is[30]

$$E_0=-S^2\sum_i z_i J_i \ , \tag{2}$$

where z_i are the coordination numbers of the lattice, which in our case is fcc. Since the antiferromagnetic arrangements used in our calculations are not eigenstates of the Heisenberg Hamiltonian we can only write down variational estimates of their exchange energies[30] and subtract them from Eq. (2). The result for such an exchange-energy difference is

$$\Delta E=-4S^2\sum_i z_i^{00} J_i \ , \tag{3}$$

where z_i^{00} gives the coordination numbers for oppositely ordered moments. These numbers are, for AF I,

$$z_i^{00}=8,0,16,0,16,0,36,\ldots \quad (i=1,2,3,\ldots)$$

and for AF II,

$$z_i^{00}=6,6,12,0,12,8,24,\ldots \quad (i=1,2,3,\ldots) \ .$$

We can use Eq. (3) to determine exchange-energy differences for AF I and AF II order from measured values of J_i and compare these with $\Delta E_{\rm I}$ or $\Delta E_{\rm II}$ listed in Table II. Exchange constants J_i have been determined for Ni_2MnSn, Cu_2MnAl, and Pd_2MnSn from neutron-scattering experiments of the spin-wave spectra[5,12,13] up to $i=6$. We thus arrive at experimental values from Eq. (3) which we give in Table IV for AF I and AF II order as $\Delta E_{\rm I}^{\rm expt}$ and $\Delta E_{\rm II}^{\rm expt}$. For convenience we repeat in Table IV our calculated values $\Delta E_{\rm I}^{\rm calc}$ and $\Delta E_{\rm II}^{\rm calc}$ from Table II. The agreement can be considered satisfactory especially in view of the large possible errors, both experimentally and numerically, and we conclude that our calculated local-density values of ΔE mainly represent exchange-energy differences that can be derived from the Heisenberg Hamiltonian.

Starting from Eq. (3) again we can proceed differently and use our calculated values for the total-energy differences $\Delta E_{\rm I}$ and $\Delta E_{\rm II}$ of Table II to determine exchange constants, and from these paramagnetic Curie temperatures. This, however, is only possible if we ignore all exchange constants except those between nearest and next-nearest neighbors, J_1 and J_2. In this case

$$\Delta E_{\rm I}=-32S^2J_1 \tag{4}$$

and

$$\Delta E_{\rm II}=-24S^2(J_1+J_2) \ , \tag{5}$$

where we may assume for S the value of $\mu_{\rm ferro}$ from Table II. For the ferromagnetic Heusler alloys we then use the well-known formula for the paramagnetic Curie temperature

$$k_B\Theta=4S(S+1)(2J_1+J_2) \ , \tag{6}$$

where k_B is Boltzmann's constant, and for antiferromagnet Pd_2MnIn,

$$k_B\Theta=-4S(S+1)J_2 \ . \tag{7}$$

Exchange constants from Eqs. (4) and (5) and paramagnetic Curie temperatures from Eqs. (6) and (7) are given in Table V together with experimental values. Table V shows that the total-energy differences allow a rough calculation of Curie temperatures with the exception of Pd_2MnSb. We believe that the remaining discrepancies are mainly due to the neglected exchange constants J_3 and J_4. The results of this subsection to us justifies the use of the modifier *local* for the Mn magnetic moments of the Heusler alloys.

TABLE IV. Energy differences ΔE from Table II, $\Delta E_{\rm I}^{\rm calc}$ and $\Delta E_{\rm II}^{\rm calc}$, and "experimental" values from Eq. (3) from exchange constants of Ishikawa (Ref. 5).

	$\Delta E_{\rm I}^{\rm calc}$ (meV)	$\Delta E_{\rm I}^{\rm expt}$ (meV)	$\Delta E_{\rm II}^{\rm calc}$ (meV)	$\Delta E_{\rm II}^{\rm expt}$ (meV)
Ni_2MnSn	−82	−72	−57	−80
Cu_2MnAl	−123	−173	−184	−172
Pd_2MnSn	−83	−66	−55	−55

IV. CONCLUSIONS

We conclude our discussion of Heusler alloys with the observation that our energy-band model of these systems does not differ in its qualitative physical content from the Hartree-Fock treatment of the so-called double-resonance Anderson Hamiltonian. This model has been studied in this context by Kim and Nagaoka,[9] Malmström *et al.*,[10] and by Price.[11] What the present work provides is a more detailed picture of the electronic structure, and the changes in the electronic structure associated with different magnetic moment alignments. The energy-band calculations show, in particular, that states lying well below the Fermi level are involved in the energy balance that determines the type of magnetic order, but that the p-d hybrid states in the immediate vicinity of E_F play a particularly sensitive role in controlling the moment loss associated with alignments other than ferromagnetic. In our view, it is these p-d states that determine the details of

TABLE V. Exchange constants J_1 and J_2 from Eqs. (4) and (5) and calculated paramagnetic Curie temperatures, Θ_{calc}, from Eq. (6) [Eq. (7) for Pd_2MnIn]. $(T_c)_{expt}$ are measured Curie temperatures and Θ_{expt} are measured paramagnetic Curie temperatures.

X_2MnY	J_1 (meV)	J_2 (meV)	Θ_{calc} (K)	$(T_c)_{expt}$ (K)	Θ_{expt} (K)
Co_2MnAl	0.840	0.062	808	697[b]	
Cu_2MnAl	0.333	0.329	691	630[c]	685[f]
Co_2MnSn	0.874	0.188	1142	829[c]	
Ni_2MnSn	0.221	−0.015	296	344[c]	337[g]
Cu_2MnSn	0.097	0.107	220	530[c,d]	
Pd_2MnIn	0.028	−0.047	42[a]	142[e]	52[h]
Pd_2MnSn	0.178	−0.019	285	189[c]	201[g]
Pd_2MnSb	0.003	0.056	53	247[c]	259[f]

[a]Calculated with Eq. (7).
[b]Webster (Ref. 4).
[c]Campbell (Ref. 3).
[d]Value uncertain.
[e]Antiferromagnetic, Campbell (Ref. 3).
[f]Webster and Ramadan (Ref. 14).
[g]Ishikawa (Ref. 5).
[h]Paramagnetic Néel temperature, Webster and Ramadan (Ref. 14).

the moment-alignment geometry. In summary then, our physical picture appears to be generally consistent with Kasuya's[8] emphasis of the lattice constant and the number of non-*d* electrons in determining the moment alignment in these alloys. We concur with this emphasis and add to it the relative importance of the *X* constituent in determining the lattice constant and the filling of the *Y*-Mn *p-d* hybrid orbitals as the more precise role of the "free" electrons of the system.

ACKNOWLEDGMENTS

The authors gratefully acknowledge many very instructive conversations concerning this material with Dr. Kiyoyuki Terakura and Dr. Thomas Penney. One of us (J.K.) would like to thank IBM World Trade Corp. for support under the visiting scientist program for the period of time during which this work was initiated. Part of this work was supported by Sonderforschungsbereich 65.

[1]F. Heusler, Verh. Dtsch. Phys. Ges. 5, 219 (1903).
[2]P. J. Webster, Contemp. Phys. 10, 559 (1969).
[3]C. C. M. Campbell, J. Phys. F 5, 1931 (1975).
[4]P. J. Webster, J. Phys. Chem. Solids 32, 1221 (1971).
[5]Y. Ishikawa, Physica 91B, 130 (1977).
[6]A. Hamzić, R. Asomoza, and I. A. Campbell, J. Phys. F 11, 1441 (1981).
[7]B. Caroli and A. Blandin, J. Phys. Chem. Solids 27, 503 (1966).
[8]T. Kasuya, Solid State Commun. 15, 1119 (1974).
[9]D.-J. Kim and Y. Nagaoka, Prog. Theor. Phys. 30, 743 (1963).
[10]G. Malmström, D. J. W. Geldart, and C. Blomberg, J. Phys. F 6, 233 (1976); F 6, 1953 (1976).
[11]D. C. Price, J. Phys. F 8, 933 (1978).
[12]K. Tajima, Y. Ishikawa, P. J. Webster, M. W. Stringfellow, D. Tocchetti, and K. R. A. Zeabeck, J. Phys. Soc. Jpn. 43, 483 (1977).
[13]Y. Noda and Y. Ishikawa, J. Phys. Soc. Jpn. 40, 690 (1976).
[14]P. J. Webster and M. R. I. Ramadan, J. Magn. Magn. Mater. 5, 51 (1977); 13, 301 (1979).
[15]P. J. Webster, J. Appl. Phys. 52, 2040 (1981).
[16]S. Ishida, J. Ishida, S. Asano, and J. Yamashita, J. Phys. Soc. Jpn. 41, 1570 (1976); 45, 1239 (1978).
[17]S. Ishida, Y. Kubo, J. Ishida, and S. Asano, J. Phys. Soc. Jpn. 48, 814 (1980).
[18]S. Ishida, S. Akazawa, Y. Kubo and J. Ishida, J. Phys. F 12, 111 (1982).
[19]W. Kohn and L. J. Sham, Phys. Rev. 140, A1133 (1965).
[20]L. Hedin and B. I. Lundqvist, J. Phys. C 4, 2064 (1971).
[21]U. von Barth and L. Hedin, J. Phys. C 5, 1629 (1972).
[22]A. R. Williams, J. Kübler, and C. D. Gellat, Jr., Phys. Rev. B 19, 6094 (1979).
[23]A. R. Williams, V. L. Moruzzi, C. D. Gelatt, Jr., J. Kübler, and K. Schwarz, J. Appl. Phys. 53, 2019 (1982); A. R. Williams, V. L. Moruzzi, C. D. Gelatt, Jr., and J. Kübler, J. Magn. Magn. Mater. 31-34, 88 (1983).
[24]Input parameters are the atomic numbers and the crystal structure ($L2_1$). The volumes of the atomic spheres are chosen to satisfy Vegard's law with compression (or dilation) being controlled by the bulk moduli of the constituent metals. Lattice constants are obtained by minimizing the total energy for each type of calculation. Ferromagnetic and antiferromagnetic moment alignments are found to have the same lattice constants.
[25]Space group and Brillouin zone of AF II Heusler alloys are those of undistorted CoO. For a description see M. R. Daniel and A. P. Cracknell, Phys. Rev. 177, 932 (1969).
[26]D. P. Oxley, R. S. Tebble, and K. C. Williams, J. Appl. Phys. 34, 1362 (1963).

[27]K. Endo, T. Ohoyama, and R. Kimura, J. Phys. Soc. Jpn. 19, 1494 (1964).
[28]N. G. Fenander, L. Wiktorin, and H. P. Myers, J. Phys. Chem. Solids 29, 1973 (1968).
[29]A. R. Williams, R. Zeller, V. L. Moruzzi, C. D. Gelatt, Jr., and J. Kübler, J. Appl. Phys. 52, 2067 (1981).
[30]N. W. Ashcroft and N. D. Mermin, *Solid State Physics* (Holt, Rinehart and Winston, New York, 1976), Chap. 33.